Thermal breaking of spanning water networks in the hydration shell of proteins

I. Brovchenko,[a] A. Krukau, N. Smolin, A. Oleinikova, A. Geiger, and R. Winter
Physical Chemistry, University of Dortmund, Otto-Hahn-Strasse 6, Dortmund D-44227, Germany

(Received 5 August 2005; accepted 20 September 2005; published online 12 December 2005)

The presence of a spanning hydrogen-bonded network of water at the surface of biomolecules is important for their conformational stability, dynamics, and function. We have studied by computer simulations the clustering and percolation of water in the hydration shell of a small elastinlike peptide (ELP) and the medium-size protein staphylococcal nuclease (SNase), in aqueous solution. We have found that in both systems a spanning network of hydration water exists at low temperatures and breaks up with increasing temperature via a quasi-two-dimensional percolation transition. The thermal breaking of the spanning water network occurs at biologically relevant temperatures, in the temperature range, which is close to the temperature of the "inverse temperature transition" of ELP and the unfolding temperature of SNase, respectively. © *2005 American Institute of Physics*. [DOI: 10.1063/1.2121708]

I. INTRODUCTION

Liquid water near a solid boundary forms one to two layers of specifically ordered water molecules. The properties of this "bound water" (orientational ordering, freezing temperature, diffusivity, etc.) differ noticeably from the properties of bulk liquid water. Near smooth surfaces, the first water monolayer forms a hydrogen-bonded network with squarelike and chainlike arrangements of molecules,[1,2] whereas the second water layer connects the specific first layer with the rest of the water, which, starting from the third layer, shows practically bulklike behavior even in the case of strongly hydrophilic surfaces.[3]

Bound water adjacent to the surface of a biomolecule is usually called hydration water or "biological" water.[4,5] This hydration water plays an important role in the conformational stability of biomolecules, their dynamics, and biological functions. In particular, both experiments and simulations[6–11] show coupled dynamics of biomolecule and its hydration water. About a monolayer water coverage is necessary to provide the native structure of the biomolecule and to restore its full dynamics.[12–15] In various biosystems the onset of the biological activity coincides with the percolation transition of water. Both experiments[16–23] and simulations[24,25] of low-hydrated biosystems show that the formation of a spanning water network occurs via a two-dimensional (2D) (strictly speaking quasi-2D) percolation transition of the hydration water at the biological surfaces. Moreover, the formation of a spanning hydrogen-bonded network of hydration water at the surface of a *single* biomolecule also occurs via a quasi-2D percolation transition.[24] Therefore, the percolation transition of hydration water corresponds to the first appearance of a "monolayer" of hydration water, which is a prerequisite for the full dynamics and function of the biomolecule. Note that the structural (and, presumably, dynamical) properties of spanning and nonspanning water networks differ clearly.[25]

Both experimental and simulation studies of the percolation of hydration water in biosystems were performed so far for low-hydrated systems only. Under full hydration conditions (i.e., in aqueous solutions), a complete monolayer of hydration water always covers the biomolecule. Taking into account the presence of a spanning network of hydration water at relatively low hydration levels, one may assume that such a network always spans the biomolecule in aqueous solution. However, as we consider the network formed by the molecules in the first hydration shell only, this is not necessarily the case. First, in dilute solutions a complete second water layer is present, which may effectively decrease the direct interconnectivity between the molecules in the first hydration water monolayer. Second, upon heating the spanning network of hydration water will ultimately break up in some temperature interval, as the number of water-water hydrogen bonds generally decreases with increasing temperature. The temperature interval, where the water network breaks, can be rather narrow, if it occurs via a percolation transition. Note that such a temperature interval is finite in any case, as the number of water molecules in the hydration shell of the biomolecule is finite (finite-size effect).

Obviously, it is difficult to study the percolation transition of hydration water or to test the spanning character of a hydration water network in aqueous solutions experimentally. However, it can be done by computer simulation, using appropriate methods to study the percolation transition at the surface of finite objects, as recently developed by us for low-hydrated systems.[24–28] To our knowledge, the breaking of the hydrogen-bonded network of hydration water with temperature was not studied even for simple systems (neither by experiments nor by simulations). Therefore, many intriguing questions remain unclear. What are the typical temperatures of the breakup of the hydration water network? How do these temperatures depend on the surface hydrophilicity and

[a]Electronic mail: brov@heineken.chemie.uni-dortmund.de

structure? These questions are of special importance in biophysics, as hydration water plays a crucial role in the function of biomolecules.

What can be the consequence of the temperature-induced breakup of the spanning hydrogen-bonded network of hydration water at the surface of a biomolecule? As hydration water strongly affects the conformation of a biomolecule, the breaking of a hydration water network may provoke some specific conformational changes of a biomolecule with temperature. If the breakup of the hydration water network occurs via a percolation transition, such conformational changes can be expected in a rather narrow temperature interval. Of course, it is interesting to compare this temperature interval with experimentally measured temperatures, where biomolecules undergo rather sharp conformational changes, such as unfolding of proteins.

Another important aspect of such an analysis is related to the possible phase separation of aqueous solutions of biomolecules. Upon heating or cooling, a homogeneous solution can separate into two coexisting phases: a water-rich phase and an organic-rich phase. The water-rich phase is usually liquid, whereas the organic-rich phase may be liquid or solid, depending on the solute and its concentration. Phase separation upon heating means the existence of a lower critical solution temperature, and deserves special interest, as it is an example of a temperature-induced macroscopical ordering of a system. In particular, such a phase transition occurs in aqueous solutions of various elastin-based polymers.[29] Temperature-induced conformational changes of biomolecules in aqueous solutions may be closely related to such a phase separation. In fact, sharp conformational changes of a single biomolecule and phase separation of the aqueous solution (which can appear as precipitation, aggregation, gel formation, etc.) usually accompany each other. Such a close relation between the conformation of molecules and a phase transition is also observed in aqueous solutions of polymers, both in experiments[30] and in some model computer simulations.[31,32]

The separation of a solution into two coexisting phases with increasing temperature means an increase of the macroscopic order (two phases appear instead of one) and, therefore, should be accompanied by an increase of entropy at the microscopic level. In the first proposed explanation of the liquid-liquid demixing of aqueous solutions with heating, an increase of entropy at the microscopic level was attributed to the breaking of highly oriented hydrogen bonds between water and solute molecules.[33] However, this physically appealing idea seems to be too simple to explain generally the phase behavior of such solutions and, in fact, may be opposed to the experimental data[34] and computer simulations.[35] Another simple approach, based on the same physical grounds, takes into consideration the ordering of the whole hydration shell of a solute molecule and imposes two states of a hydration water shell: ordered and disordered.[36,37] Obviously, not only water-solute hydrogen bonding and hydration shell formation itself, but also possible interactions between the hydrated solute (i.e., solute+hydration shell) and the surrounding solution should be taken into account.[34,38,39] In particular, at low temperatures the solution can be completely miscible due to the strong interaction of hydrated solute with water, whereas destruction of a hydration shell upon heating may provoke demixing.[40]

We may assume that the ordered state of a hydration shell, which provides strong interactions between the hydrated solute and the surrounding water, is a state, where the hydrogen-bonded network of hydration water spans the whole molecule. Accordingly, in the disordered state, the hydration shell consists of an ensemble of small water clusters and the interaction between solute and surrounding water is weak. If so, the thermal breaking of a spanning network of hydration water may be responsible for the phase separation of a solution upon heating.

Thus, the temperature-induced percolation transition of hydration water at the surface of biomolecules may have a direct relation to two important phenomena: conformational transitions of biomolecules and phase separation of their solutions, which, in turn, can be intrinsically connected. Computer simulations of phase transitions in aqueous solutions of biomolecules are not possible until now and even simulations of liquid-liquid phase transitions in aqueous solutions of simple small solutes are still difficult.[35] Therefore, currently simulations of biomolecules in water are restricted to the case of a single molecule or to the case of small clusters.

In this paper, we present the first study of the clustering and percolation transition of hydration water at the surface of single biomolecules, a small peptide and a protein, in liquid water. The process of the thermal destruction of the spanning network of hydration water is analyzed. The temperatures of the quasi-2D percolation transition of hydration water, which correspond to the breakup of the spanning network at the surface of a small elastinlike peptide (ELP) and of staphylococcal nuclease (SNase), are estimated. The results obtained are discussed in view of the experimentally observed temperature-induced conformational changes of these biomolecules and phase transitions of their aqueous solutions.

II. MODELS AND METHODS

A. Model systems and simulation details

The initial configuration of the small ELP $AceGVG(VPGVG)_3NH_2$ corresponded to the left-handed β spiral, proposed in Ref. 41. This configuration was subsequently equilibrated at $T=300$ K, first, during 30 ps in vacuum and then during 5 ns in liquid water. This equilibrated configuration was used as an initial configuration for simulations of ELP in liquid water at $T=260$, 280, 300, 320, 340, 360, and 380 K. The AMBER94 force field[42] was used for the ELP and the SPCE model[43] was used for water. The ELP molecule was placed in a cubic box with 1224 water molecules. A spherical cutoff of 9 Å was used for intermolecular interactions, and long-range Coulombic interactions were taken into account by particle mesh Ewald summation. Molecular-dynamics simulations were carried out at constant pressure ($P=1$ bar) for 360 ns. Molecular configurations were analyzed every 2 ps, i.e., 180 000 configurations were analyzed for each temperature.

The native structure of SNase was constructed using the

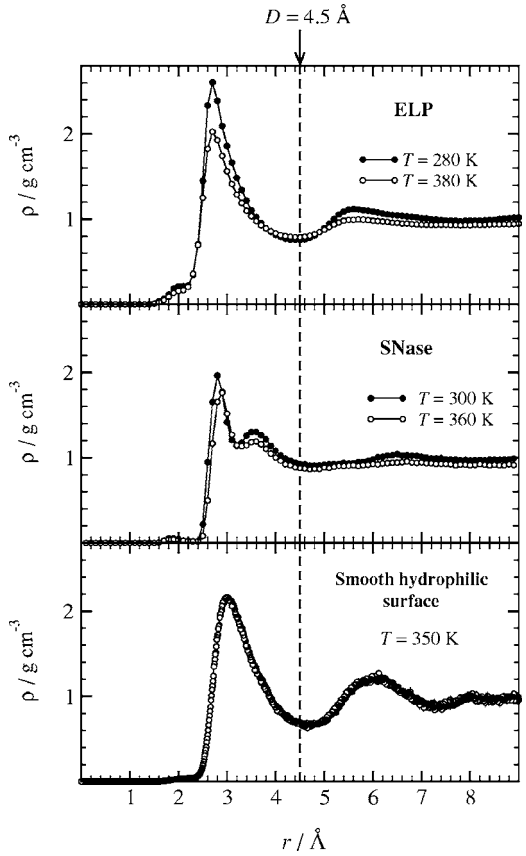

FIG. 1. Water density profiles near the surfaces of ELP (upper panel), SNase (middle panel), and near a smooth hydrophilic surface (lower panel). The vertical dashed lines show the most realistic shell width with $D=4.5$ Å.

crystallographic heavy atom coordinates from the Protein Data Bank.[44,45] The molecular-dynamics (MD) simulations were performed using AMBER6.0 with an all-atom force field[42] for SNase and the TIP3P model[46] for water (see Ref. 47 for more details). SNase was placed in a truncated octahedron box with 8604 water molecules. A spherical cutoff of 10 Å was used for intermolecular interactions, and long-range Coulombic interactions were taken into account by particle mesh Ewald summation. Constant-pressure ($P=1$ bar) MD simulations were performed at $T=300$ and 360 K during 7.2 and 9.4 ns, respectively. The last 4 ns at 300 K and the last 2 ns at 360 K were used for the analysis of configurations of hydration water every 0.2 ps.

B. Analysis of water clustering in the hydration shell

A water molecule was considered as belonging to the hydration shell, when the shortest distance between its oxygen and the heavy atoms of the biomolecule does not exceed some imposed shell width D. To find an interval of reasonable values for the width of the hydration shell, we calculated water density profiles, based on the distribution of water oxygens and hydrogens around the heavy C, N, O, and S atoms of ELP and SNase (Fig. 1, upper and middle panels), respectively. For comparison, we also show the liquid density profile of water in a cylindrical pore 12 Å radius with a moderately hydrophilic smooth surface[1,2] (Fig. 1, lower panel). It is reasonable to use the location of the first minimum of the density profile as the shell width D. Note that we neglect the shallow minimum at $r\approx 3$ Å in the case of SNase (Fig. 1, middle panel), which separates two contributions to the density profiles, originating from polar and nonpolar atoms of SNase, respectively, (see Ref. 47 for more details). For all three systems, presented in Fig. 1, $D=4.5$ Å seems to be an optimal choice for the width of the first hydration shell, which does not change noticeably with increasing temperature. Taking into account some ambiguity in the choice of D, we varied its value from 3.8 to 5.4 Å in steps of 0.1–0.2 Å. Such variations of D were also necessary for an accurate location of the percolation threshold at every temperature studied. Depending on the chosen value of D, the number N_w of water molecules in the hydration shell varied from about 80 to 170 for ELP and from about 630 to 1000 for SNase.

The existence of a hydrogen bond (H bond) between two water molecules was used as a criterion for the connectivity. Two molecules were considered as H bonded, when the distance between their oxygens did not exceed 3.35 Å for SPCE water and 3.5 Å for TIP3P water, and additionally their pair interaction energy was below −2.7 and −2.3 kcal/mol, respectively. Such criteria provide an average number of H bonds per molecule in liquid water at ambient conditions ($T=300$ K, $P=1$ bar), which is $n_H=3.3$ for both SPCE and TIP3P water models.

The analysis of water clustering and percolation was performed similarly to our previous studies of the percolation transition of water in aqueous solutions,[48,49] at smooth hydrophilic surfaces[26–28] and in low-hydrated protein systems.[24,25] The only, but important, difference in the present study was considering water clustering being exclusively established by direct H bonding between molecules in the hydration shell. To locate the percolation threshold, we studied the following properties, which characterize water clustering: the distribution n_S of clusters of size S, the probability distribution $P(S_{max})$ of the size S_{max} of the largest cluster, the mean cluster size S_{mean} (calculated after exclusion of the largest cluster), the average number n_H of H bonds per water molecule, and the fractal dimension d_f of the largest cluster (see Refs. 24, 25, 48, and 49 for more details). Please note that the latter value was calculated for SNase only, as ELP is too small for an estimation of d_f for the clusters of its hydration water.

III. PERCOLATION TRANSITION OF WATER IN THE HYDRATION SHELL OF ELP AND SNase

Various properties of water clustering in the hydration shells of ELP and SNase were studied at some fixed temperatures by varying the shell width D. Additionally, for ELP this analysis was done at a fixed shell width D with varying temperature.

A. Largest cluster size distribution

Probability distributions $P(S_{max})$ of the size of the largest water cluster in the hydration shell ($D=4.5$ Å) of the ELP molecule at various temperatures are shown in Fig. 2. The evolution of $P(S_{max})$ with decreasing temperature is quite similar to the one observed for hydration water at various

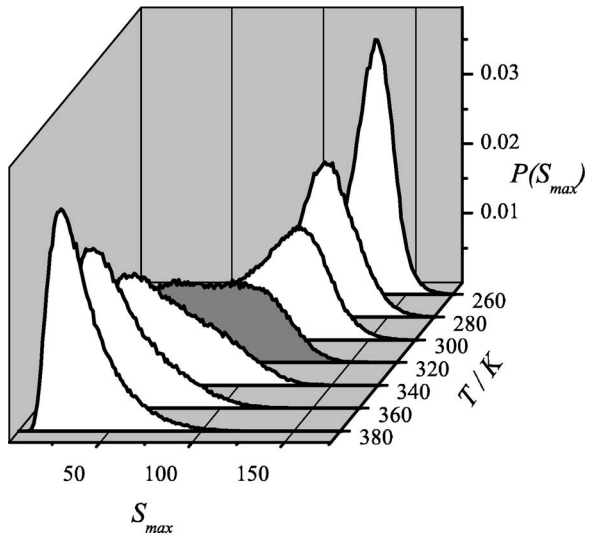

FIG. 2. Probability distribution $P(S_{\max})$ of the size $S_{\max}$ of the largest water cluster in the hydration shell of the ELP molecule (D=4.5 Å). The temperatures are indicated in the figure.

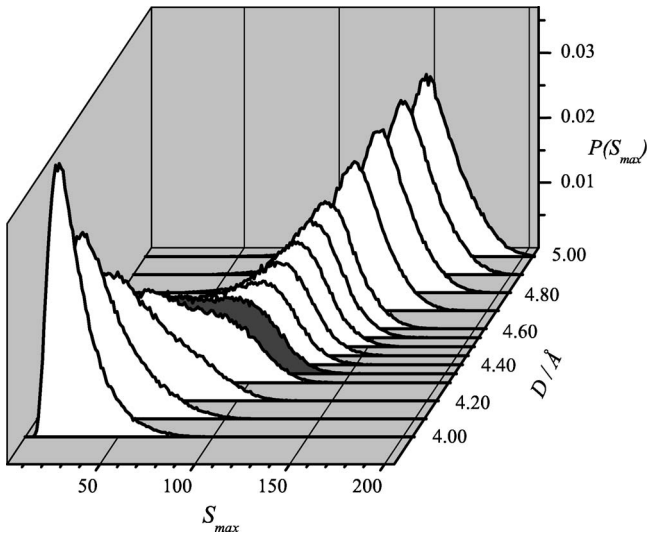

FIG. 3. Probability distribution $P(S_{\max})$ of the size $S_{\max}$ of the largest water cluster in the hydration shell of ELP (T=320 K). The widths D of the hydration shells of water are indicated in the figure.

surfaces with an increasing hydration level.[24–28] In general, the probability distribution $P(S_{\max})$ shows a two-peak structure with a left (low S) and right (high S) peak, corresponding to the nonspanning and spanning largest clusters, respectively.[27,28] This gives us the possibility to determine roughly the probability R that a spanning cluster is present in the system (spanning probability). The minimum between the two peaks of $P(S_{\max})$ approximately indicates some minimal size S', necessary for the largest cluster to be spanning, and integration of $P(S_{\max})$ for $S>S'$ yields an estimation of R.

At high temperature, spanning clusters practically never appear and nonspanning clusters dominate (Fig. 2, T=380 K, R does not exceed a few percent). With decreasing temperature, the distribution $P(S_{\max})$ shifts to higher values of S, widens, and at T=320 K exhibits a two-peak structure with approximately equal contributions from spanning and nonspanning clusters ($R\approx 50\%$). At low temperatures, the distribution $P(S_{\max})$ becomes narrower and at T=260 K a spanning cluster exists almost permanently (R approaches 100%); the largest water cluster in the hydration shell spans the whole molecule practically at any moment. A similar behavior of the distribution $P(S_{\max})$ is observed with increasing hydration shell width D, when the temperature is fixed (Fig. 3).

In accordance with the studies of the percolation transition of water at planar surfaces,[27,28] for any system size a percolation transition occurs, when the spanning probability R reaches values of about 95%. By integrating the obtained distributions of $P(S_{\max})$ from Figs. 2 and 3 for $S>S'$ we obtained R as a function of temperature and shell width, respectively, and thus could locate approximately the percolation threshold of water in the hydration shell of ELP. The thresholds obtained from the R=95% criterion are shown as open circles in Fig. 4. The vertical and horizontal error bars indicate the accuracy of the threshold values estimated from the integration of the distributions $P(S_{\max})$ of Figs. 2 and 3, respectively. As it is seen from Fig. 4, the spanning network of hydration water breaks up at about 270 K for D=4.5 Å, and this temperature increases almost linearly with an increasing shell width D. Due to the small size of the system (<200 molecules), the destruction of the spanning network of hydration water occurs in some interval of temperature or shell width. To describe this process, we determine additionally another characteristic point, corresponding to $R\approx 50\%$ (open squares in Fig. 4).

The probability distribution $P(S_{\max})$ of the size of the

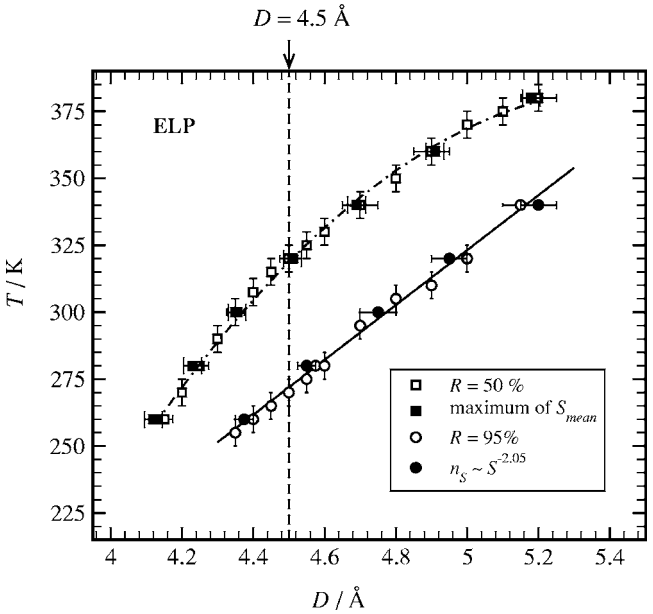

FIG. 4. Temperature of the percolation threshold of water in the hydration shell of ELP as a function of the hydration shell width D. Percolation thresholds, estimated from the distributions $P(S_{\max})$ of the largest cluster size (open circles), from the distributions n_S of the cluster size (closed circles), and linear fit of the joint data set (solid line). The shell widths, where the mean cluster size S_{mean} passes at a given temperature through a maximum, are shown by closed squares. The temperatures, where the spanning probability R, determined from the distribution $P(S_{\max})$ at a given shell width, is about 50%, are shown by open squares. The dot-dashed line is a guide for the eyes only.

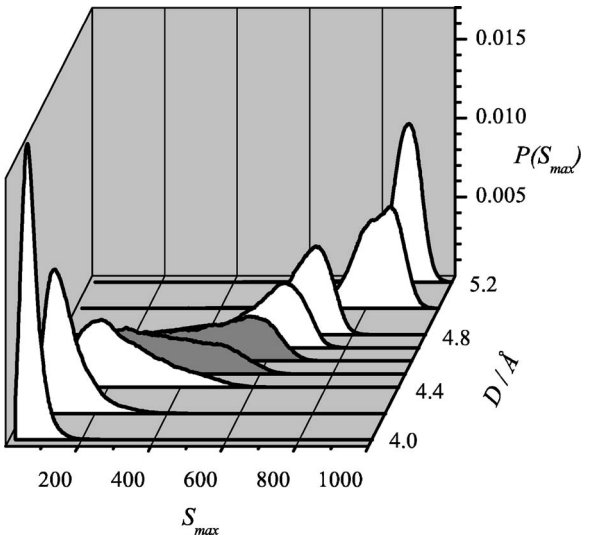

FIG. 5. Probability distribution $P(S_{\max})$ of the size $S_{\max}$ of the largest water cluster in the hydration shell of SNase ($T=300$ K). The widths D of the hydration shells of water are indicated in the figure.

largest water cluster in the hydration shell of SNase (Fig. 5) was analyzed in a similar way. At $T=300$ K, the percolation transition ($R\approx 95\%$) occurs, when $D\approx 4.80$ Å, whereas $R\approx 50\%$, when $D\approx 4.55$ Å (Fig. 6). At $T=360$ K, the corresponding threshold values of D are >5.40 Å and ≈ 5.15 Å, respectively. Note that the interval between the percolation threshold and the point, where $R\approx 50\%$, in terms of temperature or shell width, is essentially smaller in the case of SNase in comparison with the case of ELP (see Fig. 6). This is directly related to the drastically (several times) larger number of water molecules in the hydration shell of SNase.

B. Cluster size distribution

Distributions n_S of the size S of water clusters in the hydration shell of ELP at $T=280$ K and in the hydration shell of SNase at $T=300$ K are shown as a function of the shell width D in Figs. 7 and 8, respectively. At the percolation threshold, the cluster size distribution follows the power law $n_S\sim S^{-\tau}$ in the widest range of cluster sizes. The exponent τ is about 2.05 for 2D systems and about 2.2 for three-dimensional (3D) systems.[50] To locate the percolation threshold, we compared the distributions n_S with the power law $S^{-\tau}$, which is a straight line in a double logarithmic scale (Figs. 7 and 8). In both figures, the distributions n_S closest to the percolation threshold are shown by closed circles. Note that using the 3D value for the exponent τ does not affect the

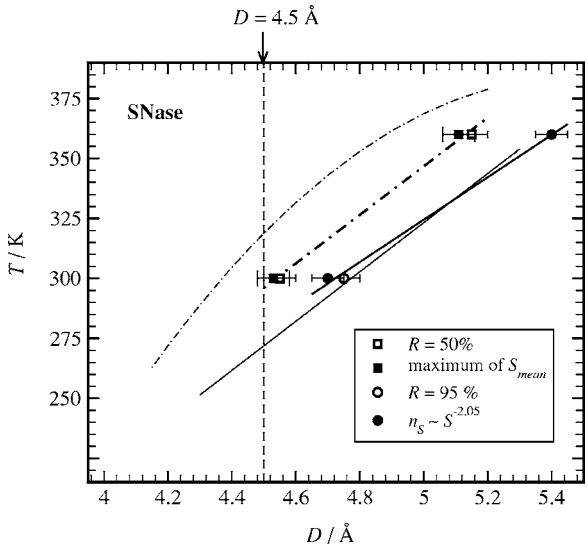

FIG. 6. Temperature of the percolation threshold of water in the hydration shell of SNase as a function of the hydration shell width D. The notation of the symbols is the same as in Fig. 4. The location of the percolation thresholds and the $R\approx 50\%$ line for the hydration shell of ELP from Fig. 4 are shown by a thin solid line and a thin dot-dashed line, respectively.

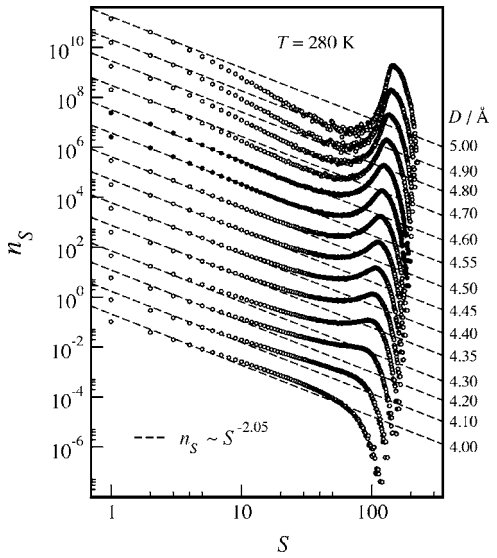

FIG. 7. Distributions n_S of the size S of the water clusters in the hydration shell of ELP at $T=280$ K for various choices of the shell width D. The distributions are shifted subsequently, starting from the bottom. The dashed lines show the power law $n_S\sim S^{-2.05}$, as expected at a 2D percolation threshold.

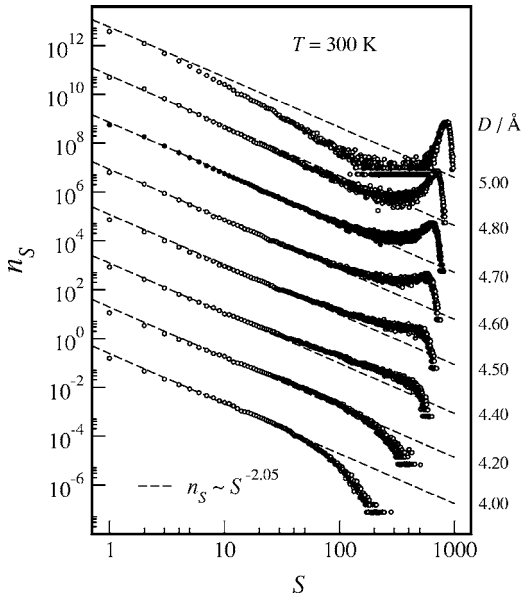

FIG. 8. Distributions n_S of the size S of the water clusters in the hydration shell of SNase at $T=300$ K for various choices of the shell width D. The distributions are shifted subsequently, starting from the bottom. The dashed lines show the power law $n_S\sim S^{-2.05}$, as expected at a 2D percolation threshold.

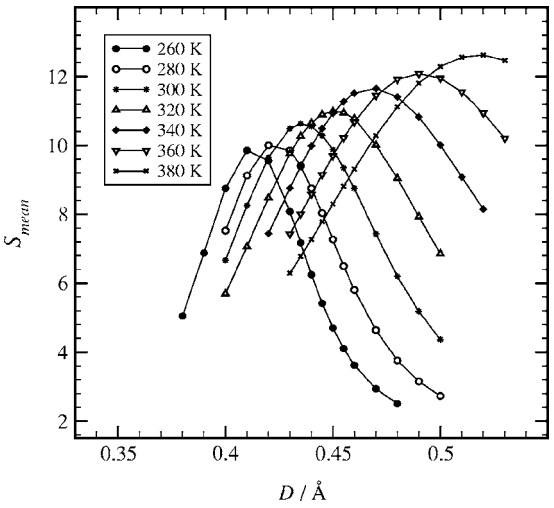

FIG. 9. Dependence of the mean size S_{mean} of the water clusters in the hydration shell of ELP on the shell width D at various temperatures.

estimation of the percolation threshold noticeably. The percolation thresholds, obtained from the analysis of the cluster size distributions, are shown by closed circles in Figs. 4 and 6 for ELP and SNase, respectively. There is a nice agreement of these percolation thresholds with the ones obtained from the distribution of the largest cluster size (closed circles in Figs. 4 and 6, see above).

C. Mean cluster size

The mean cluster size S_{mean} diverges at the percolation threshold in infinite systems and passes through a maximum when approaching the threshold in finite systems.[50] In Fig. 9 we show the dependence of S_{mean} on the width D of the hydration shell for ELP at various temperatures. Similar dependences for SNase are shown in Fig. 10. In both systems, the mean cluster size S_{mean} passes through a maximum when approaching the percolation threshold, as determined above from the distributions $P(S_{\max})$ and n_S. The maximal values of S_{mean} in the hydration shells of ELP and SNase differ by a large factor, reflecting the strong difference of the total numbers N_w of water molecules in their shells. The ratio between the maximal value of S_{mean} and N_w decreases with an increasing system size, as will be discussed below (Fig. 13). The values of the shell width D, corresponding to the maximum of S_{mean} at various temperatures, are shown as closed squares in Figs. 4 and 6 for ELP and SNase, respectively. These values are close to the ones where $R \approx 50\%$ (open squares in Figs. 4 and 5). A similar relation was observed for water clustering in low-hydrated systems.[24,27]

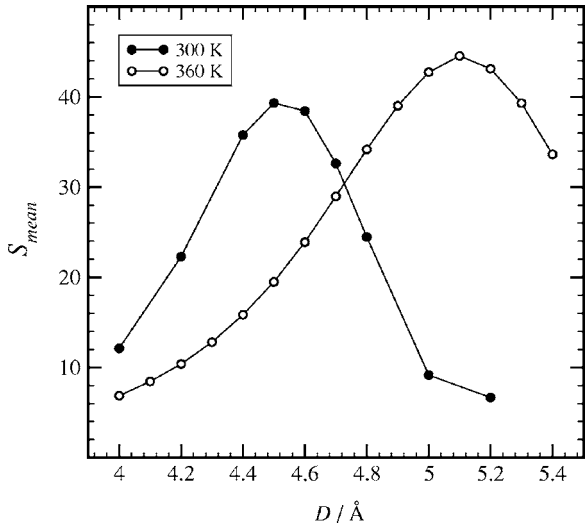

FIG. 10. Dependence of the mean size S_{mean} of the water clusters in the hydration shell of SNase on the shell width D at 300 and 360 K.

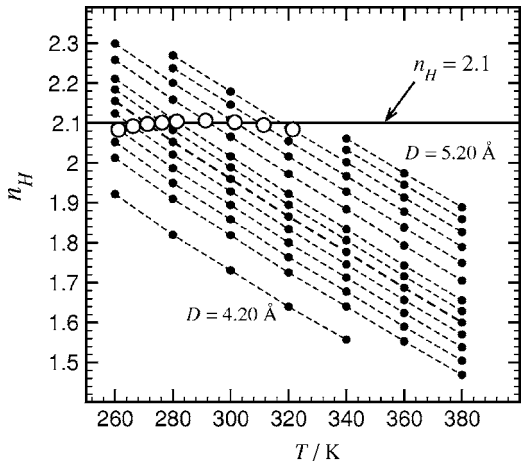

FIG. 11. Temperature dependence of the average number n_{H} of water-water hydrogen bonds between water molecules in the hydration shell of ELP for various choices of the shell width D, which increases from the bottom to the top. The open circles show the values of n_{H} at the percolation thresholds, as obtained for different D values (see solid line in Fig. 4).

D. Average number of water-water hydrogen bonds

Water clustering in various systems exhibits a highly universal behavior, when compared in terms of the average number n_{H} of water-water H bonds per water molecule. In particular, at the percolation threshold n_{H} is close to the value of 2.2 ± 0.1 for water in low-hydrated systems.[26] This value indicates that the correlated site-bond percolation of hydration water is similar to the random site or bond percolation in square and honeycomb 2D lattices with four and three neighbors, respectively.[50] The temperature dependence of the average number n_{H} of H bonds between water molecules in the hydration shell of ELP for various choices of the shell width is shown in Fig. 11 by full circles and dashed lines. The value of n_{H} at the percolation thresholds, determined from $R \approx 95\%$ criterion and from the cluster size distribution n_S, is shown in Fig. 11 by open circles. At the percolation threshold, n_{H} is about 2.1, i.e., rather close to the threshold values of n_{H} from 2.0 to 2.3 for water percolation at smooth hydrophilic surfaces and in low-hydrated lysozyme systems.[24,26] For the percolation of water in the hydration shell of SNase, we give the dependence of n_{H} on the shell width D at two different temperatures (Fig. 12, closed circles and stars). The percolation thresholds, determined from the $R \approx 95\%$ criterion and from the cluster size distribution n_S, are shown in Fig. 12 by open circles. At the percolation threshold, n_{H} is about 1.96, i.e., slightly lower than in the case of low-hydrated systems.[24,26]

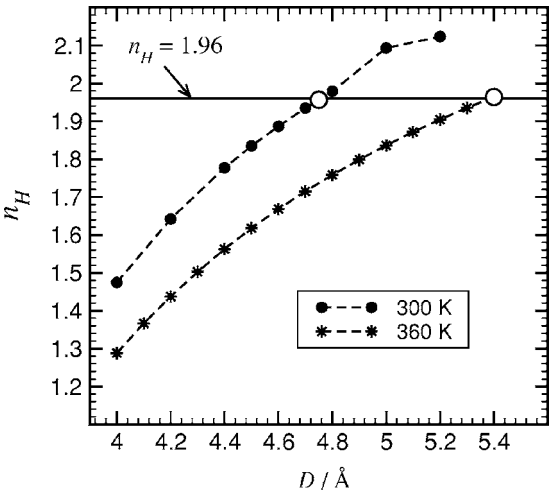

FIG. 12. Dependence of the average number n_H of water-water hydrogen bonds between water molecules in the hydration shell of SNase on the shell width D. The open circles show the values of n_H at the percolation thresholds, as obtained for both temperatures (see Fig. 6).

The highly universal description of the percolation transition in terms of the average number n_H of H bonds per water molecule can be rationalized from the behavior of the mean cluster size S_{mean}. In Fig. 13, we show the dependence of S_{mean}/N_w on n_H for all studied state points of ELP and SNase, i.e., for a wide range of temperatures and hydration shell widths D. The dependence of the normalized $S_{mean}(n_H)$ is highly universal for each system. The difference of $S_{mean}(n_H)$ for ELP and SNase is directly related to the different sizes of their hydration shells. In the larger system (SNase) the maximal value of S_{mean} is about 5% of N_w, whereas it is about 8% of N_w in the smaller system (ELP). As expected, the maximum of S_{mean} approaches the percolation threshold (vertical arrows in the Fig. 13) with an increasing system size.

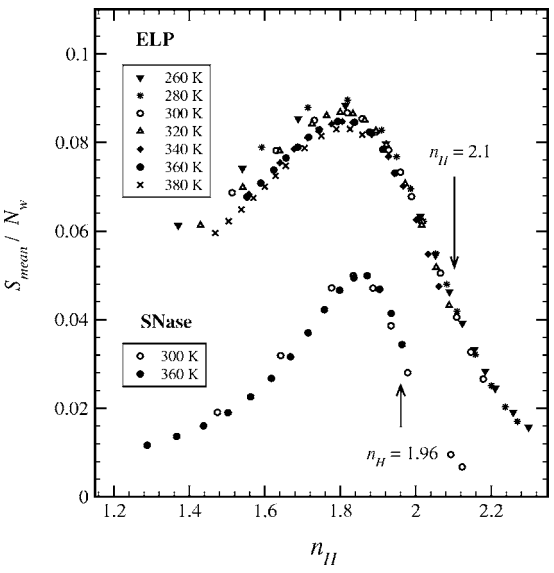

FIG. 13. Mean cluster size S_{mean} normalized by the average number N_w of water molecules in the shell as a function of the average number n_H of water-water hydrogen bonds in the hydration shell of ELP and SNase. The vertical arrows show the locations of the percolation thresholds.

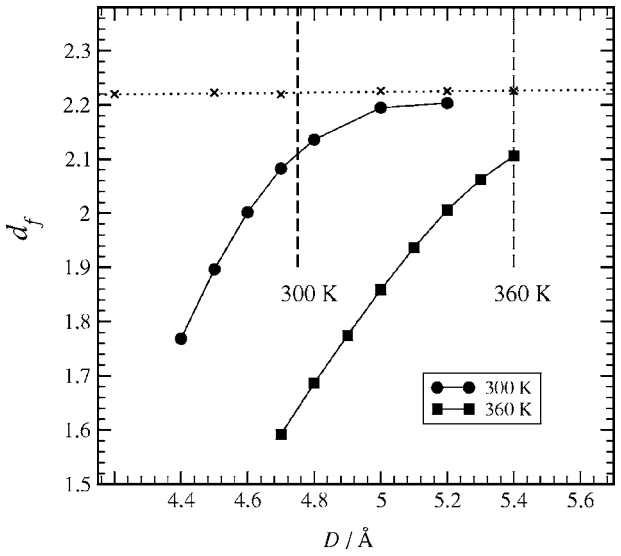

FIG. 14. Dependence of the fractal dimension d_f of the largest water cluster in the hydration shell of SNase on the shell width D at 300 and 360 K (closed symbols). The vertical dashed lines show the locations of the percolation thresholds. The crosses and the dotted line indicate the effective dimension of the water hydration shell.

E. Fractal dimension of the largest cluster

We calculated the mass distribution $m(r)$ of the molecules within the largest cluster, using each of these molecules as an origin to get reliable averages. The fractal dimension of the largest cluster d_f was obtained from fitting the mass distribution to the equation $m(r) \sim r^{d_f}$. In infinite systems, the fractal dimension of the largest cluster at the percolation threshold is determined by the system dimensionality: for 3D systems $d_f^{3D} \approx 2.53$, and for 2D systems $d_f^{2D} \approx 1.896$.[50] At the percolation threshold of water adsorbed at hydrophilic smooth planar and spherical surfaces the fractal dimension of the largest water cluster was found close to 1.9 even in relatively small systems.[27,28] In the case of low-hydrated protein systems, d_f of the largest cluster at the threshold is also about 1.9.[24]

The hydration shell of ELP is too small for a meaningful estimation of the fractal dimension of the largest cluster: even spanning clusters do not show a mass distribution $m(r)$ which can be fitted to the power law. However, this is not the case for the hydration shell of SNase, which contains several times more water molecules. We estimated the fractal dimension of the largest water clusters in the hydration shell of SNase from their mass distributions at distances between 0 and 25 Å, where they display a power-law behavior. The values of d_f, obtained from the fitting, are shown in Fig. 14. The vertical dashed lines indicate the values of D where a percolation threshold appears at 300 and 360 K, obtained from the largest cluster size distribution $P(S_{max})$ and the cluster size distribution n_S (circles of Fig. 6). The values of the fractal dimension of the largest cluster at the percolation threshold at both temperatures of $d_f \approx 2.1$ exceed the value of $d_f^{2D} \approx 1.896$. This can be attributed to the noticeable trend of the considered hydration shell towards three dimensionality due to rather large values of D or to the specific nonhomogeneous topology of the shell. We therefore calculated the

effective dimensions d of the hydration shells of various widths, taking into account all molecules in the shell (both bonded and nonbonded). The obtained value, $d \approx 2.22$, practically does not depend on temperature and only slightly increases with an increasing shell width D (see crosses and dotted line in Fig. 14). Hence, not a simple trend toward a fractal structure in 3D, but rather the specific structure of the hydration shell is responsible for the fact that the effective dimension of the water shell and the fractal dimension of the largest cluster at the threshold noticeably exceed 2 and d_f^{2D} values, respectively. Interestingly, at the percolation threshold the fractal dimension d_f of the largest cluster in the hydration shell achieves $2.10/2.22 \approx 0.946$ of the effective dimension d of the whole shell, which is extremely close to the value of $1.896/2.00 \approx 0.948$ for fractals on 2D lattices. For comparison, for 3D systems this value is about $2.53/3.00 \approx 0.843$.[50]

IV. DISCUSSION

Our simulation studies of water clustering and percolation in the hydration shell of two different polypeptides (ELP and SNase) show that at low temperatures they are covered by a spanning hydrogen-bonded network, formed by water molecules from the first hydration shell. This network includes most water molecules in the hydration shell and occupies essentially more than half of the surface of the biomolecule (see Fig. 15, upper panel). With increasing temperature, this spanning water network breaks up into an ensemble of small water clusters in the hydration shell, and even the largest water cluster occupies only a small surface area of the polypeptide (see Fig. 15, lower panel).

The transformation of a hydration water shell from a more ordered configuration with one large cluster, which spans the whole molecule, to a less ordered configuration with small water clusters only occurs via a *percolation* transition. This means that this kind of "order-disorder transformation" of the hydration shell is a transition, which occurs in a rather narrow temperature interval. Due to the finite number of water molecules in the hydration shell, such transformation is smeared out in some range of temperatures and can be characterized by the temperature dependence of a probability R to find a spanning water network. Below some low temperature, the spanning network of hydration water exists practically permanently, but when crossing the percolation threshold, the spanning probability starts to decrease sharply. For example, the percolation transition of hydration water in the shell of 4.5 Å width near ELP occurs at about 270 K (Fig. 4), i.e., below this temperature the spanning network is present in the system practically permanently. With increasing temperature, it starts to disappear and at $T \approx 320$ K its probability is about 50% only (Fig. 4). In the larger system, the monomeric protein SNase of 14 kDa molecular mass, the spanning network disappears faster with temperature. Extrapolation of the results, shown in Fig. 6, to 4.5 Å, gives a percolation threshold at about 275 K and the state with $R \approx 50\%$ at about 295 K.

As we discussed in the Introduction, the breaking of a spanning network of hydration water may be related to temperature-induced conformational transformations of biomolecules and phase separation of their aqueous solutions. We cannot say at what temperature the level of the destruction of the spanning network of hydration water is sufficient to cause such phenomena. This temperature definitely exceeds the temperature of the percolation transition of hydration water, and it is likely below the temperature, where $R \approx 50\%$. The interval between the temperature of the percolation transition ($R \approx 95\%$) and the temperature, where $R \approx 50\%$, shrinks with an increasing size of the polypeptide. For the small ELP this interval achieves 50 K (Fig. 4), whereas for the larger SNase it is only about 20 K (Fig. 6).

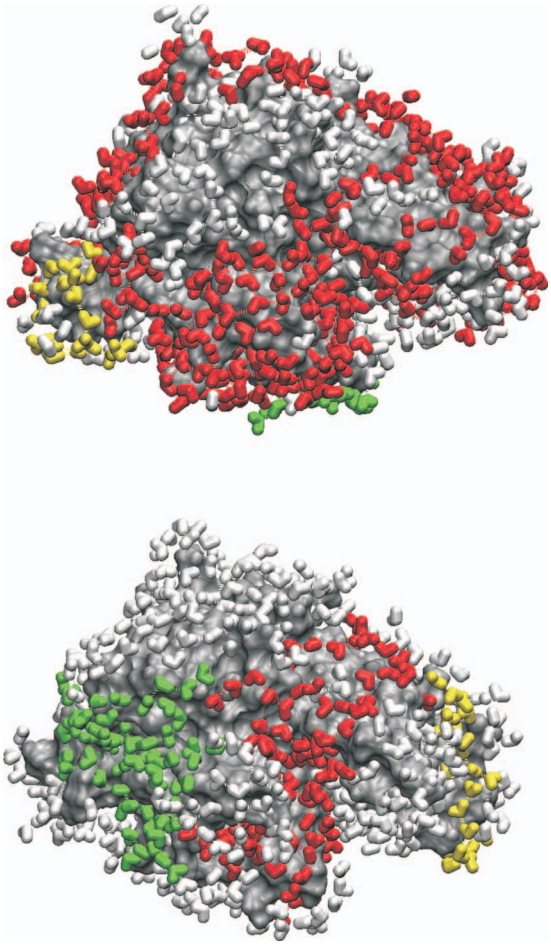

FIG. 15. (Color) Arrangement of the water molecules in the first hydration shell of SNase (shell width $D=4.5$ Å). The molecules of the first, second, and third largest hydrogen-bonded water clusters are colored in red, green, and yellow, respectively. Water molecules in smaller clusters are white. Upper panel: $T=300$ K, largest cluster is spanning. Lower panel: $T=360$ K, largest cluster is nonspanning.

A comparison of the absolute values of the temperatures of the percolation transitions of water in the hydration shells of ELP and SNase, obtained in simulations, with the real temperature scale needs special consideration. The phase diagrams of the available water models differ noticeably from the phase diagram of real water (see Refs. 51 and 52 for a comparative analysis of the phase diagrams of various water models). There are two main characteristic temperatures which can be used for estimating the temperature shift of the phase diagram of model water with the behavior of real water: the critical temperature of the liquid-vapor phase transi-

tion and the temperature of the liquid density maximum. The latter temperature is the most important parameter for our studies, as it is close to the considered temperature interval.

The SPCE water model shows the liquid density maximum at about 240 K, i.e., about 35 K below its location in real water.[52] Hence, to map approximately our results on the "temperature scale" of real water, we have to shift the data points, shown in Fig. 4, upwards by about 35 K. In this case, if we take $D=4.5$ Å, the percolation transition occurs at ~ 305 K and at $T \approx 355$ K the spanning cluster exists with a probability $\sim 50\%$. An analysis of the conformation of the peptide $GVG(VPGVG)_3$, whose hydration properties have been studied in the present paper, shows pronounced changes from a disordered to a more ordered structure at a temperature of about 290–300 K,[53] which should correspond to the interval of 325–335 K if the temperature shift between SPCE and real water is taken into account. In real aqueous solutions of large poly(VPGVG) elastin-based polymer, the phase separation into water-rich and organic-rich phases, accompanied by sharp conformational changes of the polymer (the so-called "inverse temperature transition"), occurs at about 300 K.[29] In short elastinlike peptides, where the phase separation was not detected, pronounced conformational changes of ELP molecules are still observed[54–56] and for the peptide $GVG(VPGVG)_3$ an inverse temperature transition occurs at $\sim 300-310$ K.[54,57] Hence, the experimentally measured inverse temperature transition of the peptide $GVG(VPGVG)_3$ occurs in the same temperature range, where the spanning network of hydration water breaks into an ensemble of small water clusters in our simulations. Both experimental[55,56] and simulation[56,58] studies of the even smaller GVG(VPGVG) show a conformational transition at about 310–330 K. Interestingly, the qualitative changes of the peptide-water dynamics detected in Ref. 58 at this temperature may reflect specific changes of the hydration shell.

The TIP3P water model does not show a liquid density maximum and the critical temperature of its liquid-vapor transition is not available. This essentially complicates the mapping of the results obtained for the model SNase in liquid TIP3P water, onto real systems. In general, the temperature of the liquid density maximum increases with the tetrahedral ordering of model water: usually it is overestimated for five-site water models and underestimated for three-site models (see Ref. 52 for a comparative analysis). Therefore, we may assume that the phase diagram of the three-site TIP3P water model, which shows a tetrahedral order even weaker than the SPCE model,[59] is shifted downwards by at least 35 K with respect to real water. Therefore, for a comparison with real systems, the data points for the model SNase in TIP3P water, shown in Fig. 6, should be shifted at least 35 K upwards. In this case, if we take $D=4.5$ Å, the breakup of the spanning network of hydration water occurs at $T>310$ K, and at $T>330$ K the spanning cluster exists with a probability of $\sim 50\%$. This is consistent with the experimentally observed unfolding temperature of SNase at about 325 K.[60]

The temperature of the breakup of the spanning network of hydration water depends on the definition of the hydration shell. In the present study we used the simplest possible definition, based on the distance between water oxygens and heavy atoms of the biomolecule. A more unambiguous and more physically grounded definition of hydration water should be developed for a more quantitative analysis of its percolation transition.

Summarizing, we have shown that the transformation of the hydration water shell of a polypeptide from an "ordered" to a "disordered" state occurs via a quasi-2D percolation transition, which occurs in the biologically relevant interval of temperatures. This transition may have a direct relation to temperature-induced conformational transitions of biomolecules and temperature-induced phase separations of their aqueous solutions. Further studies are necessary to clarify the observed correlation between the presence of a spanning network of hydration water and the conformational stability of a biomolecule. In this respect, studies of the effect of pressure or addition of cosolvents on the percolation transition of hydration water should be especially useful.

ACKNOWLEDGMENTS

This work was supported by the DFG Forschergruppe 436 and by the International Max Planck Research School in Chemical Biology (Dortmund).

[1] I. Brovchenko and A. Geiger, J. Mol. Liq. **96–97**, 195 (2002).
[2] I. Brovchenko, A. Geiger, and A. Oleinikova, in *New Kinds of Phase Transitions: Transformations in Disordered Substances*, Proceedings of the NATO Advanced Research Workshop, Volga River, 2002, edited by V. V. Brazhkin, S. V. Buldyrev, V. N. Rhyzhov, and H. E. Stanley (Kluwer, Dordrecht, 2002), p. 367.
[3] I. Brovchenko, A. Geiger, and A. Oleinikova, J. Chem. Phys. **120**, 1958 (2004).
[4] M. Nakasako, Cell Mol. Biol. (Paris) **47**, 767 (2001).
[5] S. Pal and A. Zewail, Chem. Rev. (Washington, D.C.) **104**, 2099 (2004).
[6] G. Phillips and B. Pettitt, Protein Sci. **4**, 149 (1995).
[7] M.-C. Bellissent-Funel, J. Mol. Liq. **84**, 39 (2000).
[8] W. Doster and M. Settles, Biochim. Biophys. Acta **1749**, 173 (2005).
[9] M. Tarek and D. Tobias, Biophys. J. **79**, 3244 (2000).
[10] A. Bizzari and S. Cannistrato, J. Phys. Chem. B **106**, 6617 (2002).
[11] S. Balasubramanian, S. Bandyopadhyay, S. Pal, and B. Bagchi, Curr. Sci. **85**, 1571 (2003).
[12] I. Kuntz and W. Kauzmann, Adv. Protein Chem. **28**, 239 (1974).
[13] J. A. Rupley and G. Careri, Adv. Protein Chem. **41**, 37 (1991).
[14] R. Pethig, Annu. Rev. Phys. Chem. **43**, 177 (1992).
[15] M. Teeter, Annu. Rev. Biophys. Biophys. Chem. **20**, 577 (1991).
[16] G. Careri, A. Giansanti, and J. Rupley, Proc. Natl. Acad. Sci. U.S.A. **83**, 6810 (1986).
[17] G. Careri, A. Giansanti, and J. Rupley, Phys. Rev. A **37**, 2703 (1988).
[18] J. Rupley, L. Siemankowski, G. Careri, and F. Bruni, Proc. Natl. Acad. Sci. U.S.A. **85**, 9022 (1988).
[19] F. Bruni, G. Careri, and A. Leopold, Phys. Rev. A **40**, 2803 (1989).
[20] M. Settles, W. Doster, F. Kremer, F. Post, and W. Schirmacher, Philos. Mag. B **65**, 861 (1992).
[21] F. Klammler and R. Kimmich, Croat. Chem. Acta **65**, 455 (1992).
[22] D. Sokolowska, A. Krol-Otwinowska, and J. K. Moscicki, Phys. Rev. E **70**, 052901 (2004).
[23] H. Haranczyk, *On Water in Extremely Dry Biological Systems* (Jagiellonian University Press, Krakow, 2003).
[24] A. Oleinikova, N. Smolin, I. Brovchenko, A. Geiger, and R. Winter, J. Phys. Chem. B **109**, 1988 (2005).
[25] N. Smolin, A. Oleinikova, I. Brovchenko, A. Geiger, and R. Winter, J. Phys. Chem. B **109**, 10995 (2005).
[26] A. Oleinikova, I. Brovchenko, N. Smolin, A. Krukau, A. Geiger, and R. Winter, Phys. Rev. Lett. (in press).
[27] A. Oleinikova, I. Brovchenko, and A. Geiger, Physica A (in press).
[28] I. Brovchenko and A. Oleinikova, "Molecular Organization of Gases and Liquids at Solid Surfaces," in *Handbook of Theoretical and Computa-*

tional Nanotechnology, edited by M. Rieth and W. Schommers (American Scientific, Stevenson Ranch, CA, in press).
[29] D. Urry, J. Phys. Chem. B **101**, 11007 (1997).
[30] S. Fujishige, K. Kubota, and I. Ando, J. Phys. Chem. **93**, 3311 (1989).
[31] G. Luna-Barcenas, J. Meredith, I. Sanchez, and K. Johnston, J. Chem. Phys. **107**, 10782 (1997).
[32] Y. Okada and F. Tanaka, Macromolecules **38**, 4465 (2005).
[33] J. Hirshfelder, D. Stevensen, and H. Eyring, J. Chem. Phys. **5**, 896 (1937).
[34] I. Brovchenko and A. Oleinikova, J. Chem. Phys. **106**, 7756 (1997).
[35] I. Brovchenko and B. Guillot, Fluid Phase Equilib. **183–184**, 311 (2001).
[36] S. Moelbert and P. D. L. Rios, Macromolecules **36**, 5845 (2002).
[37] A. Shiryayev, D. Pagan, and J. Gunton, J. Chem. Phys. **122**, 234911 (2005).
[38] I. Brovchenko and A. Oleinikova, Macromol. Symp. **114**, 223 (1997).
[39] I. Brovchenko and A. Oleinikova, High Temp. - High Press. **30**, 229 (1998).
[40] L. Aladko and Y. Dyadin, Mendeleev Commun. **4**, 67 (1994).
[41] C. Venkatachalam and D. Urry, Macromolecules **14**, 1225 (1981).
[42] W. D. Cornell, P. Cieplak, C. I. Bayly, I. R. Gould, K. D. M. Ferguson, D. C. Spellmeyer, T. Fox, J. W. Caldwell, and P. A. Kollman, J. Am. Chem. Soc. **117**, 5179 (1995).
[43] H. J. C. Berendsen, J. R. Grigera, and T. P. Straatsma, J. Phys. Chem. **91**, 6269 (1987).
[44] F. C. Bernstein, T. F. Koetzle, G. I. B. Williams, E. F. Meyerand, Jr., and M. Tasumi, J. Mol. Biol. **12**, 535 (1977).
[45] H. M. Berman, J. Westbrook, Z. Feng, G. Gilliland, T. N. Bhat, H. Weissig, I. N. Shindyalov, and P. E. Bourne, Nucleic Acids Res. **28**, 235 (2000).
[46] W. L. Jorgensen, J. Chandrasekhar, J. D. Madura, R. W. Impey, and M. L. Klein, J. Chem. Phys. **79**, 926 (1994).
[47] N. Smolin and R. Winter, J. Phys. Chem. B **108**, 15928 (2004).
[48] A. Oleinikova, I. Brovchenko, A. Geiger, and B. Guillot, J. Chem. Phys. **117**, 3296 (2002).
[49] I. Brovchenko, A. Geiger, and A. Oleinikova, Phys. Chem. Chem. Phys. **6**, 1982 (2004).
[50] D. Stauffer, *Introduction to Percolation Theory* (Taylor & Francis, London, 1985).
[51] B. Guillot, J. Mol. Liq. **101**, 219 (2002).
[52] I. Brovchenko, A. Geiger, and A. Oleinikova, J. Chem. Phys. **123**, 044515 (2005).
[53] A. Krukau, I. Brovchenko, and A. Geiger (unpublished).
[54] H. Reiersen, A. Clarke, and A. Rees, J. Mol. Biol. **283**, 255 (1998).
[55] C. Nicolini, R. Ravindra, B. Ludolph, and R. Winter, Biophys. J. **86**, 1385 (2004).
[56] E. Schreiner, C. Nicolini, B. Ludolph, R. Ravindra, N. Otte, A. Kohlmeyer, R. Rousseau, R. Winter, and D. Marx, Phys. Rev. Lett. **92**, 148101 (2004).
[57] C. Nicolini and R. Winter (unpublished).
[58] R. Rousseau, E. Schreiner, A. Kohlmeyer, and D. Marx, Biophys. J. **86**, 1393 (2004).
[59] W. Jorgensen and C. Jenson, J. Comput. Chem. **19**, 1179 (1998).
[60] R. Ravindra, C. Royer, and R. Winter, Phys. Chem. Chem. Phys. **6**, 1952 (2004).